Study of Positive Parity Band Structures in Doubly Odd ^{120}I Nucleus

A K Rana[a,b,], S, Sihotra[b*], H P Sharma[a], Renu Joshi[b], S. Jehangir[c], G.H. Bhat[d], Nazira Nazir[e], J. A. Sheikh[e], S. Rouf[c], N. Rather[c], J. Sethi[h], S. Saha[h], V. Singh[b], S. Kumar[b], N. Singh[b], J. Goswamy[b], R. Kumar[f], R.P. Singh[f], S. Muralithar[f], S. Nag[g], P. Singh[g], K. Selvakumar[g], A. K. Singh[g], R. Palit[h], and D. Mehta[b]*

[a]Department of Physics, Institute of Science, Banaras Hindu University, Varanasi, 221005 India.
[b]Department of Physics: Panjab University Chandigarh, Chandigarh, Chandigarh, 160014 India.
[c]Department of Physics, Islamic University of Science and Technology, Jammu and Kashmir, 192 122, India.
[d]Department of Physics, S.P. College, Srinagar, Jammu and Kashmir, 190001, India.
[e]Department of Physics, University of Kashmir, Srinagar-190006, India.
[f]Inter-University Accelerator Centre, New Delhi-110067, India.
[g] Indian Institute of Technology, Khargpur-110067 and
[h]Department of Nuclear and Atomic Physics, TIFR, Mumbai-400005, India.

Abstract. The band structures of the odd–odd nucleus ^{120}I were studied experimentally using the ^{11}B + ^{112}Cd → ^{120}I + 3n fusion–evaporation reaction at a beam energy of 50 MeV at the TIFR Pelletron facility. The g- g coincidence events were collected with the high-efficiency, Indian National Gamma Array (INGA), consisting of sixteen Compton-suppressed clover detectors. The present dataset enabled a significant extension of the previously known positive parity level of ^{120}I, with levels established up to ~10 MeV excitation energy. Four new γ-ray transitions were identified and placed in the level scheme and a new rotational band is also reported. Spin–parity assignments were made using Directional Correlation (DCO) ratios and polarisation (IPDCO) measurements, allowing determination of transition multipolarities In the present investigation, several positive- and negative-parity band structures are revised and on compare with the neighbouring nuclei for better understading of the positive parity state is observed in ^{120}I.

1. INTRODUCTION

The exploration of nuclear band structures remains one of the most effective tools for understanding the intrinsic properties of atomic nuclei. In particular, the investigation of doubly odd nuclei**,** which contain both an unpaired proton and an unpaired neutron, plays a vital role in elucidating the complex interplay between single-particle and collective degrees of freedom. These nuclei exhibit rich structural phenomena such as signature splitting, band crossings, shape coexistence, and chiral symmetry breaking**,** arising from residual proton-

* Corresponding author: ssihotra@pu.ac.in

neutron interactions and the coupling between the angular momenta of the odd nucleons and the collective rotation of the even–even core [1–3]. In the A ≈ 120 mass region, where the proton number lies near the magic number Z=50, the nuclear shape transitions from spherical to deformed configurations as additional valence nucleons are added. The iodine isotopes (Z = 53), in particular, occupy an important transitional zone between spherical tellurium nuclei (Z=52) and the more deformed xenon isotopes (Z = 54). This makes them an ideal testing ground for studying the competition between single-particle excitations and collective rotational motion.

The band structures of these isotopes are highly sensitive to the occupation of high-j orbitals such as $\pi g_{9/2}$, $\nu h_{11/2}$, and $\nu g_{7/2}$, which strongly influence the nuclear deformation and the alignment behaviour at high angular momenta [4,5]. The understanding of band structures of odd–odd nuclei, such as ^{118,120,122}I, is particularly challenging due to the complexity arising from the coupling of the odd proton and neutron. However, this same complexity provides a unique opportunity to probe the strength and nature of the proton–neutron residual interaction, especially in regions where both nucleons occupy orbitals near the Fermi surface. The residual interaction can lead to the formation of several possible configurations with different total angular momenta (J) resulting from the coupling of individual single-particle angular momenta (j_p and j_n). Consequently, the energy spectra of odd–odd nuclei are often rich and exhibit multiple closely spaced band structures corresponding to different configurations and deformations [6,7].

The iodine isotopes in the A=110–130 mass region have been extensively studied through fusion–evaporation reactions and in-beam γ-ray spectroscopy. These studies have revealed a variety of rotational bands associated with quasiparticle excitations in the $\pi g_{9/2}$ and $\nu h_{11/2}$ orbitals [8–10]. The experimental investigations on neighbouring isotopes such as ^{117}I, ^{119}I, and ^{121}I [11–13], have provided valuable information on the centrifuged coupling of the odd proton with the even-even ^{118}Te core [14]. In ^{120}I, the nuclear structure becomes even more interesting because of its position near the midshell, wherein the influence of both proton and neutron shell effects is significant. The unpaired proton in the $g_{9/2}$ orbital and the unpaired neutron in the $h_{11/2}$ or $g_{7/2}$ orbital give rise to several possible configurations leading to multiple rotational bands. The competition between these configurations at various spin states leads to band crossings and alignment phenomena, which provide information on the single-particle energies and pairing correlations. Furthermore, at moderate to high spins, the breaking of Cooper pairs and the gradual alignment of angular momenta result in back-bending or smooth band crossings, features that have been widely observed in this mass region [15,16].

2. Experimental Details

High-spin states in the odd–odd nucleus ^{120}I (Z = 53, N = 67) were populated through the fusion evaporation reaction,

$$^{112}\text{Cd}(^{11}\text{B},3n)^{120}\text{I@50MeV} \quad (2.1)$$

using a ^{11}B ion beam delivered by the Pelletron-LINAC accelerator at the Tata Institute of Fundamental Research (TIFR), Mumbai. The beam energy was 50 MeV, optimized to favour the 3n evaporation channel for the production of ^{120}I at moderate angular momentum. A ^{112}Cd target with a thickness of approximately 3 mg/cm² was prepared on a 8 mg/cm² thick lead (Pb) backing to ensure complete stopping of the recoiling nuclei within the target material. The target was of natural isotopic composition, containing small fractions of ^{114}Cd and ^{116}Cd isotopes, though the dominant contribution originated from ^{112}Cd. The de-excitation γ-rays emitted from the reaction residues were detected using the Indian National Gamma Array

(INGA), a high-efficiency γ-ray detection system comprising 16 Compton-suppressed clover-type high-purity germanium (HPGe) detectors [17-19]. Each clover detector consists of four closely packed HPGe crystals surrounded by bismuth germinate (BGO) anti-Compton shields, which significantly reduce background noise arising from Compton scattering.
The typical photopeak efficiency of the array is about 5% at 1.33 MeV (for ^{60}Co), assuming all 24 clover detectors are operational. In this experiment, 16 detectors were used, positioned at various angles (Two-dimensional angular correlation matrices between the detectors at 90° and those at 32° and 148° were constructed.) relative to the beam axis to enable angular correlation and polarization measurements. The detectors were operated in addback mode, combining coincident energy deposits from adjacent crystals to enhance photopeak efficiency especially for high-energy γ-rays above ~1 MeV. Efficiency calibration of the array up to 3 MeV was carried out using standard ^{133}Ba and ^{152}Eu radioactive sources. The experimental data were collected using a digital data acquisition system based on Pixie-16 modules manufactured by XIA LLC, [17]. These modules allowed event-by-event recording of γ-ray energies and timestamps with high precision. Two-fold and higher-fold coincidence events were recorded, resulting in an exceptionally large dataset containing approximately 1.1×10^{10} γ–γ and 3.2×10^{8} γ–γ-γ coincidence events. Data sorting was performed using the MARCOS (Multi-Parameter time-stamped based Coincidence Search) software, developed at TIFR. The program sorts the time-stamped events to generate E_γ–E_γ matrices and E_γ–E_γ–E_γ cubes, compatible with the Radware software [20] suite for subsequent offline analysis.
The present work has been presented earlier [21].
The γ–γ coincidence matrices were created by shorting the least data introduced to establish coincidence relationships among transitions and to construct the level scheme of ^{120}I. The energies of intense γ-rays were measured with an accuracy better than ±0.3 keV, whereas weak or high-energy transitions carried uncertainties up to ±0.7 keV. The relative γ-ray intensities were determined with uncertainties of about 5% for γ-rays below 1 MeV, increasing to 10% for higher energies [14,22].

2.1 Angular Correlation and Polarization Measurements

The spin–parity (J^π) assignments of the excited levels and the multipolarity of γ-ray transitions were deduced from Directional Correlation of Oriented states (DCO) and Integrated Polarization Directional Correlation (IPDCO) measurements. Two-dimensional DCO matrices were constructed using events detected by clover detectors placed at 90°, 32°, and 148° with respect to the beam axis. Gates were set on known stretched E2 transitions (such as the 368 keV and 898 keV transitions) to extract DCO ratios. For the INGA geometry, an ideal DCO ratio of approximately 1.0 or greater indicates a quadrupole (E2) transition, while values ≤ 0.6 suggest dipole (M1) character. Transitions with DCO ≈ 1.0 can also correspond to pure ΔI = 1 dipole transitions [23]. For polarization measurements, the clover detectors at 90° were employed as Compton polarimeters. The IPDCO [24], technique involves constructing two asymmetric matrices corresponding to the parallel (N∥) and perpendicular (N⊥) scattering directions relative to the reaction plane. The polarization asymmetry parameter (Δasym) was calculated as:

$$\Delta_{asym} = \frac{a(E_\gamma)N_\perp - N_\parallel}{a(E_\gamma)N_\perp + N_\parallel} \quad \text{.....(2.2)}$$

Where *a(Eγ)* is an energy-dependent correction factor that accounts for the intrinsic asymmetry of the detector response. A positive Δ_asym value corresponds to an electric transition (E-type), while a negative value indicates a magnetic transition (M-type).

3. RESULTS AND DISCUSSION

The present study on the nucleus ^{120}I report the positive parity states above built upon the above 10+ state at 1008 keV, consistent with earlier studies [25,26,20]. The revised level structure has been established up to an excitation energy of approximately 10 MeV, as illustrated in fig. 1**,** where the observed levels are systematically arranged into several rotational bands, designated B9–B12 for clarity. This level scheme shows noticeable differences from the one reported previously [26]. In the present analysis, the sequence of γ-ray transitions was determined based on detailed γ–γ coincidence relationships, energy summations, and relative intensity measurements. Some weak transitions, for which placement could not be confirmed with certainty, are indicated as dashed lines in the level diagram. Additionally, the present results differ from the more recent findings of Moon *et al.* [27], where supplementary data were included to support the reported level scheme. The discrepancies between the current and earlier schemes primarily arise from the improved experimental sensitivity achieved in this study. The use of the Indian National Gamma Array (INGA**)**, with its enhanced photopeak efficiency and large coincidence dataset**,** enabled the detection of weak γ transitions that were not observed in previous investigations, thereby allowing a significant extension of the known level scheme [17].

Band B9

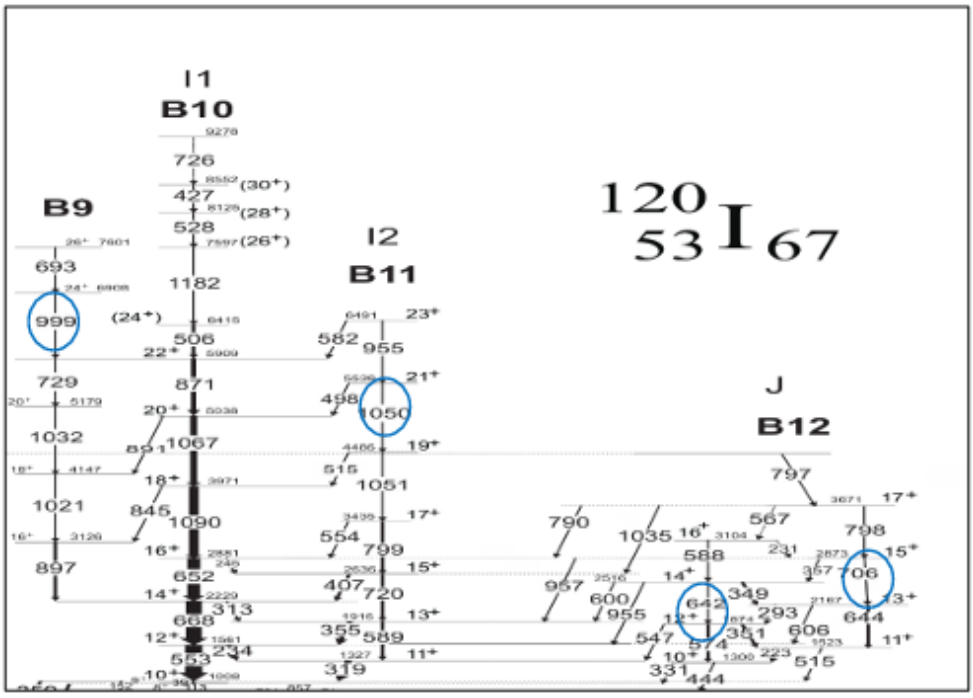

Fig.1. Partial Level scheme of ^{120}I showing the parity levels. Energies of γ-rays and levels are given in keV. The width of the arrow representing the γ-transition indicates relative intensity of the γ-ray.

A new transition 693 keV is identified on the top of band B9, hence band as updated up to state $I^{\pi}=26^{+}$, In this study suported double energy gate of 897/sum (553+668+897+1021+1032+729+999+69) shows in fig.2.

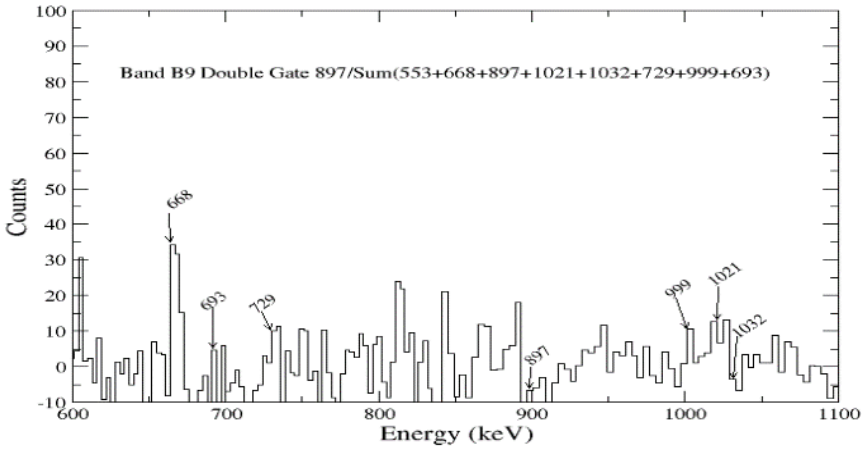

Fig.2 The observed of 693 keV transition of band B9 double gate 897/sum (553+668+897+1021+1032+729+999+693 keV).

A detailed inspection of the level spacing reveals significant structural evolution at higher spin. The energy interval between the 14^+ and 16^+ levels shows a sudden compression, indicating a deviation from regular rotational behavior. This effect is interpreted as evidence of the alignment of a pair of $g_{7/2}$ protons, a process observed in neighbouring isotopes as well. Beyond this point, irregularities in level spacing up to the 26^+ state indicate an additional alignment of two $h_{11/2}$ neutrons, consistent with the breaking of neutrons pairs at higher angular momentum.

Band B10

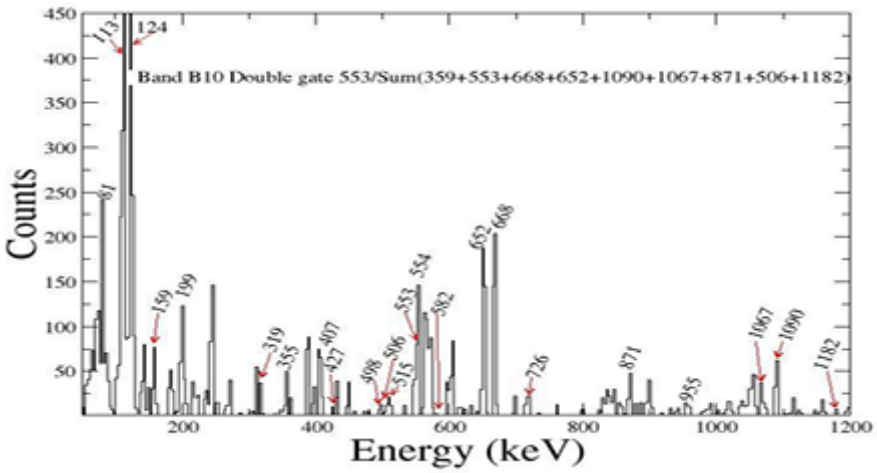

Fig. 3. Shown Energy spectrum of band B10 double gate 553/sum (359+553+668+652+1090+1067+871+506+1182 keV).

Band B10 was the yrast band populated structure in the present experiment and represents the principal positive-parity sequence in ^{120}I. Earlier investigations by Kaur *et al.*[25].

assigned this band to a $\pi g_{7/2} \otimes \nu h_{11/2}$ configuration ; however, later work by Moon *et al*. reinterpreted it as arising from a $\pi h_{11/2} \otimes \nu h_{11/2}$ configuration [27]. This revised assignment is now widely accepted for ^{120}I and neighboring odd–odd iodine isotopes [26, 29-30].
The present analysis supports this configuration, which effectively explains the band's alignment behavior and energy systematics. The alignment plots are generated for $I^{\pi}=10^{+}$ state which is yrast in structure of ^{118,120,122}I nuclei in order to understand the role of neutron-proton alignments. The back-bending is observed around frequency 0.34 MeV in case of ^{122}I, but not in case of lighter isotopes of ^{118,120}I as shown in fig.4. Such beahaviour clearly suggests that neutron pair is strongly bound below the subshell gap at N=68. In this study, four new energy levels linked by four new γ transitions were identified above the previously known 506 keV transition shown in fig.3 and extending the band upto an excitation energy of ~10 MeV. Furthermore, the energy spectrum gated on the 553 keV transition displays a stronger intensity for the 1182, 528, 427, and 726 keV transitions above the gate than for the 506 keV transition below [30]. This anomalous intensity pattern indicates that the state de-excited by the 506 keV γ-ray has a long lifetime, suggesting the presence of an isomeric level within the band. The R_{DCO} ratios of $\Delta I = 2$ and $\Delta I = 1$ transitions are approximately ~ 1.0 and ~ 0.5, respectively, while the 506 keV transition yields a value of 1.1(2), intermediate between these limits. This ambiguity prevents a definitive multipolarity assignment, but given the isomeric behavior, the 506 keV transition is tentatively identified as a stretched E2 transition, implying a (24^{+}) isomeric state at the top of the band [27,26]. The configuration of the bandhead can thus be associated with $\pi[h_{11/2}\ (g_{7/2})^2\ ]23/2^{-} \otimes \nu[(h_{11/2})^3]27/2^{-}$, corresponding to the full alignment of the valence nucleons outside the ^{114}Sn core [32].

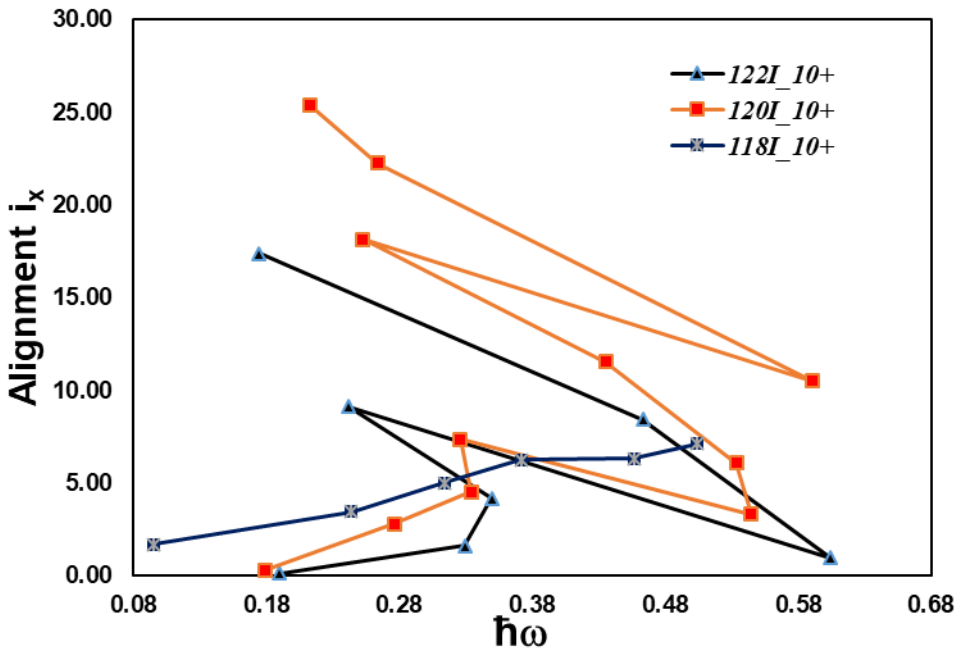

Fig.4. Plots of the spin alignment in for the rotatioal bands in ^{118,120,122}I. A rotational reference with the Harris parameters $J_0 = 15\ \hbar^2\ MeV^{-1}$ and $J_1 = 25\ \hbar^4 MeV^{-3}$ has been subtracted.

Band B11

Band B11, identified as the signature partner of the yrast band B10, was previously established up to the (17^+) level [28,26]. In the current work, this band has been extended up to the 23^+ state through the addition of higher-spin transitions, clarifying its relationship to the main positive-parity sequence. The previously ambiguous 1051 keV [28] transition was confirmed to be a doublet. The strong correlation between Bands B10 and B11 in terms of energy spacing and $\Delta I = 2$ cascade structure reinforces their identification as signature partners originating from the same quasiparticle configuration ($\pi h_{11/2} \otimes \nu h_{11/2}$) [26,27,31]. The consistent alignment behaviour of both sequences across increasing rotational frequencies suggests that the underlying configuration is stable across the observed spin range, though slight variations in moment of inertia reflect subtle differences in the coupling of the odd proton and neutron.

Band B12

Band B12, which is relatively weakly populated in this reaction, was previously established up to the (15^+) level [31,26]. In the present study, one additional transition at 798 keV has been observed, extending the sequence to higher spin. Furthermore, a 797 keV interband transition connecting Band B12 to Band B6 (negative parity band structures levels are not shown in fig.1) has been firmly identified through coincidence spectra. This interconnection provides further evidence for the coexistence of positive- and negative-parity structures at high excitation energy in ^{120}I [20,26,31]. Given its proximity in excitation energy and transition pattern to Bands B10 and B11, Band B12 may represent either a signature or configuration partner of these bands. However, its weak population precludes a definitive structural assignment at this stage. The band is most likely associated with the same underlying $\pi h_{11/2} \otimes \nu h_{11/2}$ configuration [31], but populated through a less favorable reaction channel or higher-order feeding transition.

4. Conclusion

The experimental evidence collectively supports a consistent description of the positive-parity rotational structures in ^{120}I. Bands B10 and B11 form a robust signature-doublet pair based on the $\pi h_{11/2} \otimes \nu h_{11/2}$ configuration, exhibiting systematic alignment behaviour characteristic of $h_{11/2}$ quasiparticle couplings. The newly observed branch within Band B10 reveals competing $g_{7/2}$ proton and $h_{11/2}$ neutron alignments**,** a feature also seen in neighbouring nuclei. Band B12, though weakly populated, likely shares a similar configuration and may indicate the onset of additional quasiparticle excitations at higher spin. The suggesting the influence of a high-K component in the bandhead structure. These findings together provide important insights into the evolution of quasiparticle alignments and the competition between proton and neutron configurations in triaxially deformed odd–odd nuclei near $A \approx 120$ mass region.

Acknowledgement

Authors acknowledged the joint effort of IUAC, New Delhi, TIFR, Mumbai, UGC-DAE CSR and SINP, Kolkata, for establishing the INGA clover array. The authors would like to thank the IUAC Pelletron staff for their help and efforts for smooth functioning of the accelerator. Financial support from DST, and IUAC (Project No. IUAC/UFR-72303) New Delhi, under the Center of Advanced Study Funds, is duly acknowledged. Financial support under the CSIR (project No. 42-809/201803(1443) /18/EMR-II), and DST(SERB-

CRG/2022/000239) New Delhi, is duly acknowledged. UGC-NFSC-SRF fellowship Ref. No. 20160035694 (for AK Rana) is duly acknowledged and also thankful to BHU for Grant (R/Dev/D/IOE/incentive/2022-23/47643). The authors (GHB, JAS, SJ, NR) would like to acknowledge Science and Engineering Research Board (SERB), Department of Science and Technology (Govt. of India) for providing financial assistance under the Project No.CRG/2019/004960 to carry out a part of the present research work.

References

1. R. Bengtsson and S. Frauendorf, *Nucl. Phys. A* 327, 139 (1979). https://doi.org/10.1016/0375-9474(79)90322-1
2. P. Möller and J. R. Nix, *At. Data Nucl. Data Tables* 26, 165 (1981). https://doi.org/10.1016/0092-640X(81)90003-6
3. S. Frauendorf, *Rev. Mod. Phys.* 73, 463 (2001). https://doi.org/10.1103/RevModPhys.73.463
4. A.K. Jain, R.K. Sheline, D.M. Headly, *Rev. Mod. Phys.* 62, 393 (1990). https://doi.org/10.1103/RevModPhys.62.393
5. G.D. Dracoulis et al., *Phys. Rev. C* 44, R1246 (1991). https://doi.org/10.1103/PhysRevC.44.R1246
6. J.H. Hamilton, *Prog. Part. Nucl. Phys.* 35, 635 (1995). https://doi.org/10.1016/0146-6410(95)00048-N
7. A. Bohr and B.R. Mottelson, *Nuclear Structure*, Vol. II (Benjamin, New York, 1975). https://inis.iaea.org/records/t5zg3-rdz45
8. R. Muralithar et al., *Phys. Rev. C* 95, 024320 (2017). https://doi.org/10.1103/PhysRevC.95.024320
9. Y.K. Gupta et al., *Eur. Phys. J. A* 54, 91 (2018). https://doi.org/10.1140/epja/i2018-12526-2
10. J.A. Cameron et al., *Nucl. Phys. A* 465, 501 (1987).
11. E S Paul et al., Phys. G. Nucl. Pan Phys. 19 913-919 (1993). https://doi.org/10.1088/0954-3899/19/6/011
12. C. Wheldon et al., *Phys. Rev. C* 63, 011304 (2001). https://doi.org/10.1103/PhysRevC.63.011304
13. C. B. Moon et al., Eur. Phys. J. A 5, 13–16 (1999). https://link.springer.com/content/pdf/10.1007/s100500050251.pdf
14. S. Juutinen, *Phys. Rev. C,* 61, 014312 (1999). https://doi.org/10.1103/PhysRevC.61.014312
15. K. Starosta et al., *Phys. Rev. Lett.* 86, 971 (2001). https://doi.org/10.1103/PhysRevLett.86.971
16. I. Ragnarsson, *Phys. Lett. B* 264, 5 (1991). https://doi.org/10.1016/0370-2693(91)90693-K
17. R. Palit et al., Nucl. Instrum. Methods A 90, 680 (2012). https://doi.org/10.1016/j.nima.2012.03.046
18. K. Starosta et al., Nucl. Instrum. Methods A 423, 16 (1999). https://doi.org/10.1016/S0168-9002(98)01220-0
19. R.K. Bhowmik et al., *Eur. Phys. J. A* 14, 93 (2001). https://link.springer.com/article/10.1007/s12043-001-0163-0
20. C. B. Moon et al., Phys. Lett. B 782, 602 (2018). https://doi.org/10.1016/j.physletb.2018.06.008
21. A. Kumar et al., Proceedings of the DAE Symp. on Nucl. Phys. 68 (2024) https://www.sympnp.org/proceedings/68/A144.pdf

22. D. C. Radford, Nucl. Instrum. Methods A 361, 306 (1995). https://cds.cern.ch/record/274799/files/SCAN-9501125.pdf
23. A. Kramer-Flecken et al., Nucl. Instrum. Methods A 275, 333 (1989). https://doi.org/10.1016/0168-9002(89)90706-7
24. K. Starosta et al., Nucl. Instrum. Methods A 423, 16 (1999). https://doi.org/10.1016/S0168-9002(98)01220-0
25. H. Kaur et al., Phys. Rev. C 55, 512 (1997). https://doi.org/10.1103/PhysRevC.55.512
26. L. I. Li, et al., Chin. Phys. Lett. 30, 062301 (2013). https://doi.org/10.1088/0256-307X/30/6/062301
27. C. B. Moon et al., J. Korean Phys. Soc. 59, 1525s (2011). https://scholar.kyobobook.co.kr/article/detail/4040060019664
28. H. Kaur et al., Z. Phys. A: Hadrons Nucl. 352, 11 (1995). https://link.springer.com/article/10.1007/BF01292755
29. P. Singh, B. Ding, Y. Zheng. *et al.,* Phys. Rev. C, 85, 034319. (2012). https://doi.org/10.1103/PhysRevC.85.034319
30. Liu, G. Y., Yao, S. H., Ding, B., & Zheng, Y., Chin. Phys. Lett., 29, 092301 (2012). https://doi.org/10.1088/0256-307X/29/9/092301
31. K. Starosta, T. Koike,, C. J. Chiara, *et al*., Nucl. Phys. A, 682, 375. (2001). https://doi.org/ 10.1016/S0375-9474(00)00663-1
32. J. Gableske , A. Dewald, et al., Nucl. Phys. A 691, 551–576 (2001). https://doi.org/10.1016/S0375-9474(01)00564-4